Frequency-Domain Photon Migration Measurements for Quantitative Assessment of Powder Absorbance: A Novel Sensor of Blend Homogeneity†

RAJESH R. SHINDE, G. V. BALGI, S. L. NAIL,‡ AND E. M. SEVICK-MURACA*

Contribution from *The Photon Migration Laboratory, School of Chemical Engineering, Purdue University, West Lafayette, Indiana 47907-1283.*

Received March 15, 1999. Accepted for publication August 3, 1999.

Abstract □ The measurement and analysis of frequency-domain photon migration (FDPM) measurements of powder absorbance in pharmaceutical powders is described in the context of other optical techniques. FDPM consists of launching intensity-modulated light into a powder and detecting the phase delay and amplitude modulation of the re-emitted light as a function of the modulation frequency. From analysis of the data using the diffusion approximation to the radiative transport equation, the absorption coefficient can be obtained. Absorption coefficient measurements of riboflavin in lactose mixtures are presented at concentrations of 0.1 to 1% (w/w) at near-infrared wavelengths where solution absorption cross sections are difficult to accurately measure using traditional transmission measurements in nonscattering solutions. FDPM measurements in powders enabled determinations of absorption coefficients that increase linearly with concentration (w/w) according to Beer–Lambert relationship. The extension of FDPM for monitoring absorbance of low-dose and ultralow-dose powder blending operations is presented.

1. Introduction

The blending of powders of differing particle size, density, shape, and surface characteristics can result in demixing and segregation phenomenon that can have a critical impact on pharmaceutical powder blending and tableting processes. Indeed, the complexity of the blending process and the uncertainty in assessment of spatial homogeneity of the active agent in the powder bed within the blender are especially crucial in low dose (<1% w/w) or ultralow-dose (<0.1% w/w) formulations involving high potency pharmaceutical compounds. While much progress has been made toward a better physical understanding of the complexities involved in powder blending, measurements which validate the end point of a mixing process and provide assurance of the blend homogeneity remain as missing tools required to better address the quality assurance issues facing the pharmaceutical industry. In 1993, the "Barr decision" highlighted the litigious nature of incomplete knowledge of powder blending and sampling operations that could impact the uniformity of pharmaceutical tablets. Furthermore, the decision underscored the necessity for a measurement technique that (i) provides assessment of blend homogeneity, (ii) minimizes the error associated with powder sampling, (iii) provides sampling size measurements reflective of no more than three unit dosages and, (iv) enables real time measurements of blend homogeneity during the mixing operation. Currently, the "gold-standard" measurement of blend homogeneity rests with "thief sampling" combined with HPLC or other wet chemistry analysis. The typical sampling "thief" consists of an inner cylinder with sampling compartments along its axis and an outer, rotating, hollow cylinder stamped with apertures that permit flow into the inner sampling chambers when both cylinders are properly aligned. The difficulties associated with thief sampling are (i) the induced variance error associated with uneven flow of differing sized particles into sampling chambers, (ii) the disturbance of powder bed by the insertion of the thief, and (iii) the inability to make in situ, real time variance measurements, σ_m^2, related to actual variance in drug concentrations, σ_d^2, during the blending operation. It should be emphasized that the measured variance, σ_m^2, reflects a contribution from sampling, σ_s^2, analysis, σ_a^2, and drug concentration, σ_d^2, variances, i.e., $\sigma_m^2 = \sigma_s^2 + \sigma_a^2 + \sigma_d^2$. The Barr decision stipulates the largest sample volume for analysis must be less than three times that of a single tablet.

Numerous investigators have sought to develop techniques to assess the blend homogeneity without the need to remove a sample from the powder bed, thereby eliminating the influence of sampling error or variance, σ_s^2. In a system to model blend homogeneity, Muzzio and coworkers[1] have developed a technique to investigate the blending phenomenon that involves solidification of the contents of a mixing vessel and slicing cross sections of the solid mixture for image analysis. The blend homogeneity is then studied by using statistical methods to assess the mixing of differently colored glass beads in the size range of tens of microns. Their technique to assess mixing in a model system is static, and restricted to a specific model system of glass beads, yet provides a means for assessing measured variances independent of σ_s^2, and aids in building process models for validation of powder mixing.

Other investigators have sought optical means to assess blend homogeneity. Diffuse-reflectance fiber optic probes are being investigated extensively for evaluating powder characteristics.[2,3] Using near infrared (NIR) fiber optics reflectance from powders, Cho et al. (1997)[4] measured

* To whom correspondence should be directed. Phone: 765-496-2377. Fax: 765-494-0805. E-mail: sevick@ecn.purdue.edu. http://photon.ecn.purdue.edu/~chepmi/ppml.html.

† Supported by the Purdue NSF I/UCRC in Pharmaceutical Processing.

‡ School of Pharmacy.

10.1021/js990079+ CCC: $18.00
Published on Web 09/08/1999

derivative spectra from backscattered light in the wavelength range between 1100 and 2500 nm to measure blend homogeneity of a lactose, microcrystalline cellulose, and sodium benzoate mixture based on its variance as a function of mixing time. Since the spectra can be measured in situ, the sampling variance arises only from the volume of powders probed in the diffuse backscattered light and is not impacted by the powder flow problems associated with a sampling thief. Their results suggest that backscatter techniques using fiber optics can interrogate 0.154 to 0.858 g of powder with a standard deviation of 0.16 g. Arguing that single doses range from 0.1 to 1.0 g, these investigators contend that the backscatter technique fits the regulatory requirements for probing 0.3 to 3.0 g of total tablet mass. Analysis of diffuse reflectance and backscatter measurements often assumes wavelength-independent scattering so that variance of the derivative spectra is assumed to be a measure of the variance of light-absorbing constituents in the blend. Unfortunately, the assumption of wavelength-independent scattering is not always correct, and monitoring spectral derivatives for blend homogeneity studies may not always be a prudent approach for minimizing artifact.

In this contribution, we introduce the techniques of frequency-domain photon migration for assessment of blend homogeneity and demonstrate its applicability for determination of powder absorbance for pharmaceutical process monitoring. In contrast to diffuse reflectance and backscatter measurement and analysis currently pursued for such applications, FDPM is based upon the *time-dependent diffusive* scattering of light. Owing to the measurement approach, the variance of analysis and measurement are minimized when compared to thief sampling and time-invariant diffuse reflectance or backscatter techniques, respectively. In the following, we briefly review the theory describing light transport in powders and describe the inherent difficulties associated with time-invariant measurement of diffuse reflectance. We describe the physics of FDPM measurements as well as the instrumentation and analysis of measurements and present FDPM absorbance values of riboflavin in lactose powders to demonstrate the feasibility of the technology. Finally, we comment upon the diagnostic ability of FDPM for pharmaceutical monitoring of intermediate and final powder-based products.

2. Light Transport in Powders

Optical techniques for monitoring the absorbance associated with active ingredients in a powder bed are typically based upon diffuse reflectance or backscatter techniques that employ a constant intensity source of broadbeam illumination or a point source illumination via fiber optic coupling. Analysis of backscatter or diffuse reflectance are typically employed using empirically based chemometric analyses or physically based radiative transfer equations and associated assumptions. Since chemometrics is beyond the scope of this contribution, we refer the reader to a treatise on the subject by Muhammad and Kowalski[5] and Adams.[6] Instead, in this contribution we are concerned with extraction of the absorption coefficient, $\mu_a(\lambda)$, at wavelength λ, within the powder bed. Assuming that the absorption coefficient is the sum of different light absorbing species, i.e., $\mu_a(\lambda) = \Sigma_i \epsilon_{\lambda,i}[C_i]$, measurements made at multiple wavelengths enable determination of concentration of the light absorbing components from the simultaneous solution of a series of linear equations. However, as briefly described below, it is difficult and in some approaches impossible to determine absorption coefficients independently from first-principles data analyses of time-invariant, reflected light.

Radiative Transfer of Light in Scattering Media—Light propagation is ubiquitously described by the radiative transfer equation (RTE), that can be solved with proper boundary conditions to predict the radiance, L, [Watts/(m^2 sr)] associated with light traveling in direction of unit vector $\hat{s}$ per unit solid angle.

$$\frac{1}{c}\frac{\partial L(\bar{r},\hat{s},t)}{\partial t} + \bar{\nabla} L(\bar{r},\hat{s},t)\hat{s} = -(\mu_s + \mu_a)L(\bar{r},\hat{s},t) + \mu_s \int_{4\pi} L(\bar{r},\hat{s}',t) f(\hat{s},\hat{s}') d\Omega' + Q(\bar{r},\hat{s},t) \quad (1)$$

Briefly, the first and second terms on the left hand side of eq 1 describe the accumulation of radiance (where c is the speed of light in the medium), and the net rate of increase of radiance associated with light traveling in direction $\hat{s}$, respectively. The first term on the right hand side denotes the loss mechanisms whereby light traveling in direction $\hat{s}$ is lost through absorption and scattering out of direction $\hat{s}$. Here, μ_s and μ_a [1/(length)] are the linear scattering and absorption coefficients, respectively. The second term describes a "gain term" by which light traveling all directions $\hat{s}'$ (or solid angle $\hat{\Omega}'$) is scattered into the preferred direction $\hat{s}$. To properly account for this "inscattering," into direction $\hat{s}$, the phase function, $f(\hat{s}',\hat{s})$ must be known. $f(\hat{s}',\hat{s})$ describes the probability of photons traveling in direction $\hat{s}'$ being scattered into direction $\hat{s}$ and must satisfy the relation:

$$\int_{4\pi} f(\hat{s},\hat{s}') d\Omega' = 1 \quad (2)$$

$Q(\bar{r},\hat{s},t)$ represents the source term for the photons traveling in direction $\hat{s}$.[7−10]

Diffusion Approximation to RTE—The typical powder bed of micron-sized particles scatters light multiple times in all directions. Integration of eq 1 over all possible solid angles, Ω, leads to the equation of continuity shown below.

$$\frac{1}{c}\frac{\partial \phi(\bar{r},t)}{\partial t} + \bar{\nabla}\bar{j}(\bar{r},t) = -\mu_a \phi(\bar{r},t) + S(\bar{r},t) \quad (3)$$

where

$$S(\bar{r},t) \equiv \int_{4\pi} Q(\bar{r},\hat{s},t) d\Omega,$$

$$\phi(\bar{r},t) \equiv \int_{4\pi} L(\bar{r},\hat{s},t) d\Omega$$

and

$$\bar{j}(\bar{r},t) \equiv \int_{4\pi} L(\bar{r},\hat{s},t)\hat{s}\, d\Omega$$

$S(\bar{r},t)$ is an isotropic source term, $\phi(\bar{r},t)$ is the angle-independent fluence rate, and $\bar{j}(\bar{r},t)$ is the photon flux.

The *diffusion approximation*, which assumes weak angular dependence of radiance, $L(\bar{r},\hat{s},t)$, and predominant scattering such that $\mu_a \ll (1 - g)\mu_s$, is typically valid in powders. Specifically, in the standard diffusion approximation, the angular radiance, $L(\bar{r},\hat{s},t)$, is expressed as a sum of the angle independent fluence rate, $\phi(\bar{r},t)/(4\pi)$, and a small directional flux, $3/(4\pi)\hat{s}\cdot\bar{j}(\bar{r},t)$. Details regarding the diffusion approximation as well as higher order approximations to the RTE are available in literature[11,12] and not described here for brevity. Nonetheless, the optical diffusion equation derived from RTE describing the angle-independent fluence of light $\phi(\bar{r},t)$(W/m^2) is written as:

$$D\nabla^2\phi(\bar{r},t) - \mu_a\,\phi(\bar{r},t) = \frac{1}{c}\frac{\partial\phi(\bar{r},t)}{\partial t} - S(\bar{r},t) \qquad (4)$$

where

$$D \equiv \frac{1}{3[(1-g)\mu_s + \mu_a]} \equiv \frac{l_{tr}}{3}.$$

D is the optical diffusion coefficient (cm), g is the average cosine of the scattering angle and the term $(1-g)\mu_s$ is the isotropic scattering coefficient. l_{tr} is the transport mean free path of the diffusing photon. Equation 4 can be solved for different boundary conditions (see section 3). However, the diffusion theory has limitations. The diffusion theory assumes that the radiance is nearly isotropic in its angular dependence and the sources are isotropic. These conditions are satisfied in strongly scattering situations, i.e., $\mu_a \ll (1-g)\mu_s$, and far from the boundaries and sources. The minimum distance from the source and boundaries at which light is detected must be at least greater than $10l_{tr}$ without having to resort to higher order approximations. As described in the section below, the diffusion equation can be solved for incident intensity-modulated light to enable determination of absorption independently of scattering properties and without the need to know scattering phase functions.

3. Frequency Domain Photon Migration

The technique of frequency-domain photon migration depends upon launching intensity modulated, monochromatic light at modulation frequencies ranging from 100's of kHz to 100's of MHz. As the resulting "photon-density wave" propagates through the scattering media, its amplitude is attenuated and it is phase-delayed relative to the incident light. The transport of photons via FDPM in the media can be treated as a diffusive process. The light detected in reflectance or transmittance mode is modulated at the same frequency as that of the incident light. This light is found to be phase-shifted, θ', and its amplitude attenuated by a factor M relative to the incident light. Measurements of θ' and M are acquired at different modulation frequencies, $\omega/2\pi$, of the source. The solution of the diffusion equation (section 2) is used to relate the phase-shift, θ', and amplitude modulation attenuation, M, to the two separate optical properties of the powder, the absorption coefficient, μ_a, and the isotropic scattering coefficient, μ'_s. The advantages of FDPM are twofold: first, these measurements do not require an external calibration, and second, the absorption and isotropic scattering coefficients are obtained as separate parameters rather than as a single product (as determined in continuous wave measurements analyzed with multiflux approximations to the radiative equation).

3.1. Theory of FDPM—The measurements described herein were conducted with the frequency-domain photon migration apparatus illustrated in Figure 1. The light source was a 670 nm laser diode (150 mW) which was sinusoidally modulated at the frequency of interest by modulation of the current input. The light from the laser sources was split so that approximately 10% of the light was collected by a reference photomultiplier tube (Hamamatsu R928, Hamamatsu, Japan) via a 1000 μm optical fiber. The remaining transmitted light was launched into the lactose–riboflavin powder mixture using a 1000 μm source optical fiber positioned flush with the wall of the sample container. The scattered light from the powder was detected by another 1000 μm optical fiber that was mounted at known distances away from the source fiber, also flush

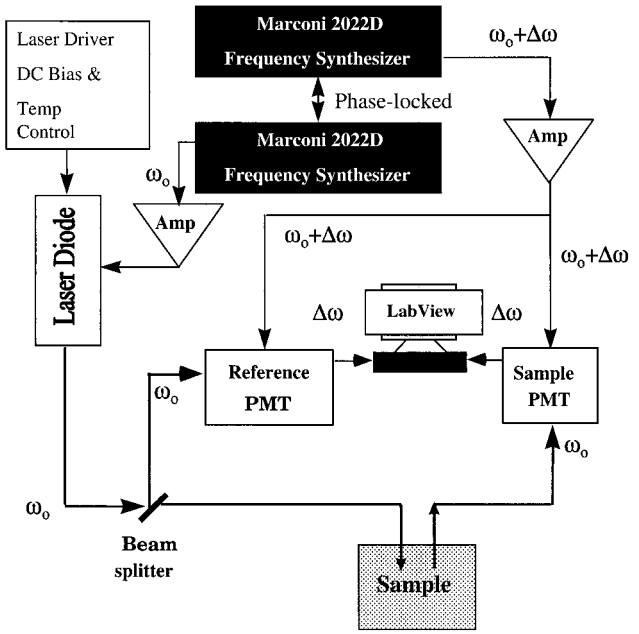

Figure 1—A schematic of an experimental setup of the frequency domain photon migration (FDPM). The light source is a laser diode, but can be substituted with a Ti:sapphire laser.

with the wall of the container. The other end of this detecting optical fiber was directed to a second photomultiplier tube. The source and detector fibers were maintained in a coplanar geometry. Estimates of the isotropic scattering and absorption coefficients using the phase-difference and amplitude modulation data were obtained by regression from analytical solutions to the optical diffusion equation described below. The relative separations between the source and detector fibers were chosen such that the distances between them were at least 10 isotropic scattering mean free paths l^* (or $1/\mu'_s$) to ensure multiple light scattering. The photomultiplier tubes (PMT's) were gain modulated at a modulation frequency, $\omega/2\pi$, of the laser diode plus an offset frequency ($\Delta\omega/2\pi$) of 100 Hz. This standard heterodyne technique yielded a 100 Hz signal at the photomultiplier output from which the phase shift, θ', and modulation, M, could be extracted. A data acquisition software (Labview 4.01, National Instruments) was customized to acquire and process the experimental data.

A pulsed light source was also employed for the frequency-domain studies enabling us to interrogate the samples with a Ti:sapphire system at other wavelengths. The source was a tunable 2 ps pulsed optical train output of a Tsunami picosecond-pulsed titanium–sapphire (Ti:sapphire) laser (Model 3950B, Tsunami, Spectra Physics, CA) pumped by a 10 W argon-ion laser (Beamlok 2060, Spectra Physics). Near infrared wavelengths of 750 and 820 nm were generated using this Ti:sapphire laser. The Ti:sapphire laser pulse train was delivered at a repetition rate of 4 MHz with an average output power level of 20 mW. The light was delivered to the powder mixtures in the same manner as that for the 670 nm laser diode. For the Ti:sapphire light source, PMT gain modulation was achieved at a harmonic of the pulsed laser repetition rate plus the 100 Hz offset frequency. Details of the instrumentation have been discussed elsewhere.[13]

The experimentally measured quantities were the phase lag, θ', at the detector relative to a reference signal as a function of modulation frequency, ω. To nullify instrument responses (i.e., phase delays induced by instrumentation), measurements at multiple detector positions were used to determine relative phase shifts ($\Delta\theta'_{rel}$).

3.2. Prediction of FDPM Measurements—For photon diffusion in an infinite medium, the optical diffusion equation (section 2) has been solved to obtain analytical expressions for different boundary conditions.[11,14] The following solutions for infinite and zero boundary conditions have been obtained by Haskell et al.

Zero Boundary Condition—The zero boundary condition sets the fluence rate, ϕ, to zero at the physical boundary. This condition was found suitable for our experimental setup. The solution for the diffusion equation with this boundary condition leads to the following expression for $\Delta\theta'_{rel}$.

$$\Delta\theta'_{rel}(\lambda) = |d_1 - d_2|k_{imag} - \arctan\left(\frac{k_{imag}}{k_{real} + \frac{1}{|d_1 - d_2|}}\right) \quad (5)$$

where

$$k_{imag} = \sqrt{\frac{3}{2}\mu_a\mu'_s\left(\left(1 + \left(\frac{\omega}{\mu_a c}\right)^2\right)^{1/2} - 1\right)}$$

and

$$k_{real} = \sqrt{\frac{3}{2}\mu_a\mu'_s\left(\left(1 + \left(\frac{\omega}{\mu_a c}\right)^2\right)^{1/2} + 1\right)}$$

$$k = k_{real} + ik_{imag}$$

where d_1 and d_2 are the two source-detector positions, λ is the wavelength of light in vacuum, and c is the speed of light in the continuous medium. k is the wavenumber which has a real component, k_{real}, and an imaginary component, k_{imag}. The experimental data of phase-shift versus modulation frequency was then fit to eq 5 using a Marquardt–Levenberg nonlinear regression algorithm to yield independent parameter estimates of the absorption coefficient, μ_a, and the isotropic scattering coefficient, μ'_s. The measured variance in θ' at different frequencies was less than 1%.

The volume sampled by diffusing light depends upon the absorption and scattering properties of the powder. The average distance traveled by photons into the powder bed from the light source can be calculated from the approach developed by Sevick et al.[15] The fluence of the photons is determined at various points in the powder bed, and the amount of photons detected at various source-detector separations is calculated. The average distance of travel of photons into the powder increases with separation, and then drops off. For example, in these set of measurements at source-detector separations of 0.55 and 1.22 cm, and for a scattering coefficient of 120.0 cm^{-1}, and an absorption coefficient of 0.02 cm^{-1}, the average distance that the photons traveled into the powder bed are 0.44 and 0.50 cm respectively. Assuming a spherical profile of the photons propagating in the powder bed, the volume sampled does not exceed more than 0.5 cm^3. We can see that the volume probed by this technique is not very large, and is well within the sampling volume limit.

4. Experimental Section

Materials—In order to demonstrate the ability to detect small changes in absorbance, we chose to employ riboflavin/lactose powder mixtures as a model system. Lactose monohydrate USP was supplied by Sheffield, Inc. (Norwich, NY), and riboflavin USP was provided by Hoffmann LaRoche Laboratories Inc. (Nutley, NY). Both materials were used as received. In the following, we describe measurements of riboflavin and lactose absorption cross section using conventional attenuation measurements in dilute nonscattering solutions, as well as by FDPM techniques.

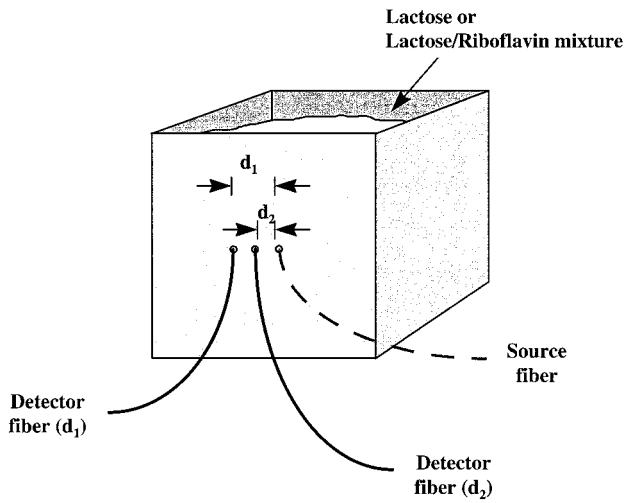

Figure 2—An illustration of the sample box used for making FDPM measurements on lactose–riboflavin mixtures.

4.1. Absorption Coefficient of Riboflavin Solution—The extinction coefficient for riboflavin (molecular weight = 376.4) was measured using a Perkin-Elmer UV-vis spectrophotometer. Riboflavin is sparingly soluble in water; hence, in order to facilitate the dissolution of riboflavin, sodium hydroxide solution was added dropwise until a clear solution was obtained. The solution was centrifuged to remove debris. A stock solution was prepared with riboflavin concentration of 0.014 g/L. The samples were prepared 1 h prior to experiments, because riboflavin is unstable in solution and the instability increased with increasing sodium hydroxide concentrations. The measurements were accomplished on the stock solution and dilutions of the stock solution of 1:2 and 1:5 by deionized water. The absorption spectra was obtained at wavelengths ranging from 200 to 900 nm scanned at a rate of 240 nm/minute. The extinction coefficient of a light-absorbing species in a mixture is determined from the Beer–Lambert's law, $(1/l)\log_{10}(I_o/I) = \mu_a(\lambda) \equiv \epsilon(\lambda)[C]$, where μ_a is the absorption coefficient of the solution, I_o is the incident light, I is the detected light passing through a sample of thickness l. C denotes the concentration of the absorbing species, i.e., riboflavin, in the solution. $\epsilon(\lambda)$ is the extinction coefficient of the species and can be obtained for a particular wavelength by measuring the absorption coefficient (μ_a) at various concentrations. The slope of the straight line fit to the data provides the extinction coefficient.

4.2. Extinction Coefficient of Lactose-Riboflavin Mixtures—The extinction coefficients for various lactose–riboflavin mixtures were obtained for wavelengths ranging from 350 to 470 nm. Riboflavin content in the lactose varied from 0 to 1.0 wt %. The powder samples were dissolved in deionized water, and their absorption coefficient was obtained at different riboflavin concentrations. The slope of the straight line fit gave the extinction coefficient of the total lactose–riboflavin mixture.

4.3. Absorption Coefficients and Extinction Coefficients of Lactose–Riboflavin Powder Mixtures by FDPM—In order to measure the isotropic scattering and absorption coefficient of the powder mixtures, the samples were placed in a rectangular box. Three optical fibers were inserted into one side of the box and the tip of the fibers were flush with the interior side of the box as shown in Figure 2. Such an arrangement prevented movement of the

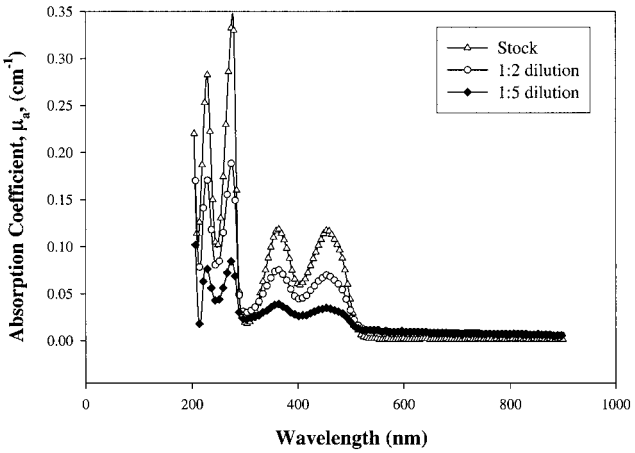

Figure 3—Absorption spectra obtained at three dilutions of a riboflavin stock solution of 0.0372 mM in deionized water. The dilutions were effected in the ratios of (i) 1:1 (0.0186 mM), (ii) 1:2 (0.0124 mM), and (iii) 1:5 (0.0062 mM) with deionized water. The wavelengths scanned were from 200 to 900 nm.

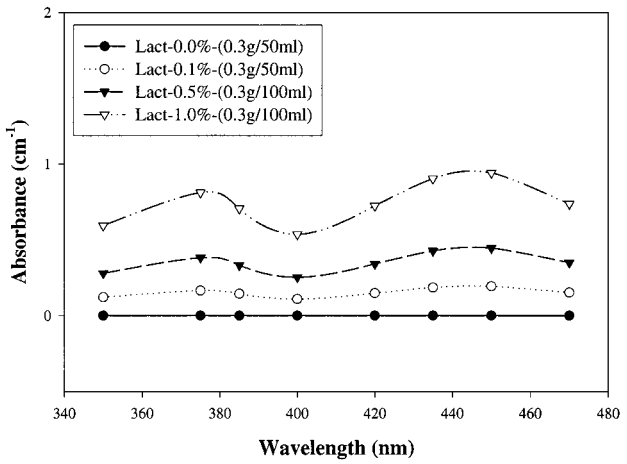

Figure 4—Absorption spectra of four dissolved lactose–riboflavin mixtures. Measurements were accomplished from 350 to 475 nm. Riboflavin concentrations ranged from 0 to 1 wt % for the four powders. The symbols denote the concentrations of the four powder mixtures dissolved in deionized water. Lines are spline fits to the data.

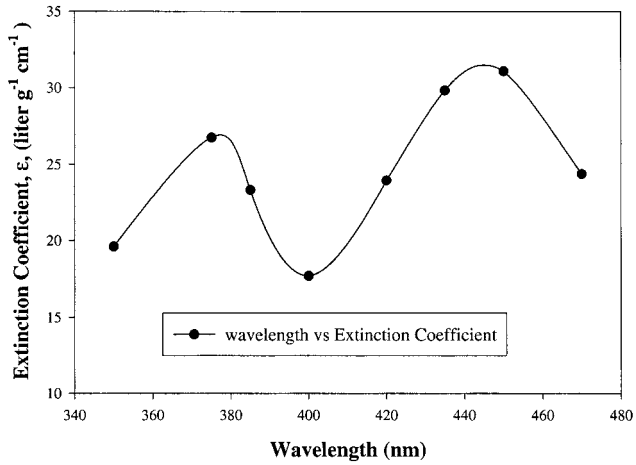

Figure 5—Plot of the extinction coefficients of riboflavin calculated from the experimentally measured absorption coefficients at wavelengths from 350 to 475 nm, using a UV-spectrophotometer. The UV extinction coefficients for lactose were negligible and hence neglected. The symbols represent the calculated extinction coefficients, and the lines are spline fits to the data.

powder arising due to insertion of fibers or probes. One fiber delivers monochromatic light from the laser source, and the scattered light is collected by the other two fibers. All the fibers were of the same length, and the fiber separations were 0.55 and 1.22 cm. In order to eliminate instrumentation errors, the relative phase shifts between the two detector positions were measured by taking the difference of the measured phase shifts for each position d_1 and d_2. The fibers could be used in any combinations as source and detectors. The powder mixtures were poured into the box (5.7 × 7.2 × 7.6cm), and measurements were carried out without any compaction of the powders. The powders were mixed in a V-blender, in batches of 250 g.

FDPM measurements were accomplished on four different powder mixtures. The four mixtures were lactose with 0, 0.1, 0.5, and 1 wt % riboflavin mixed uniformly in a blender. Riboflavin absorbs strongly at 470 nm. Extensive trial runs were carried out to determine the scattering and absorption coefficients of the powder mixtures at different wavelengths. Initially, modulated light at wavelengths of 488 and 515 nm was used. At these wavelengths, a good signal could be detected for the pure lactose powder. However, the lactose powder containing riboflavin tended to absorb a substantial amount of light, causing a significant attenuation of the amplitude and preventing an accurate measurement of the phase-delay, θ'. As a result, FDPM measurements were conducted at wavelengths of 670 nm and higher, away from the absorbance maximum of riboflavin. At these wavelengths and smaller absorption cross sections, absorption by the riboflavin does not predominate and FDPM provided accurate signals for determination of powder optical properties. The two other wavelengths of light used were 750 and 820 nm.

It is noteworthy that the FDPM technique is capable of measuring small changes in the absorbance of the powders, due to the absorption by riboflavin.

5. Results and Discussion

5.1. Absorption Coefficient of Riboflavin Solution—Figure 3 shows a plot of the absorption spectrum of riboflavin in alkaline solution. As can be seen from the figure, there is significant absorption in the UV range from 300 to 500 nm. Two peaks are observed in the spectra at around 360 and 480 nm. The absorption drops to negligible values beyond 500 nm, thus providing only a small window for measuring riboflavin concentrations. Owing to the small absorption cross section of the riboflavin at wavelengths greater than 500 nm, it is not possible to accurately detect solution riboflavin concentrations outside the UV range.

5.2. Extinction Coefficient of Lactose−Riboflavin Mixtures—On the basis of these results, further measurements were made on lactose−riboflavin mixtures in the UV range 350 to 470 nm. The mixtures were dissolved in deionized water in concentrations ranging from 3 to 6 g/L. Lactose dissolves very easily in water and does not show any detectable absorption in the UV range that was studied. Results are presented in Figure 4. It can be seen that as the riboflavin content in the lactose is increased from 0 to 1% (by weight) at constant lactose concentration, the absorption spectra shows two peaks originating at the same wavelength ranges (360 and 480 nm) as those for pure riboflavin (Figure 3). The results from Figure 4 were then utilized to calculate the extinction coefficient of riboflavin in the powder mixtures at different wavelengths. The slope of a straight-line plot of the absorbance for the solutions of the mixtures at different riboflavin concentration gave the extinction coefficient of riboflavin. The extinction coefficients thus determined for riboflavin in the powder mixtures at different wavelengths are plotted in Figure 5.

5.3. Absorption Coefficients and Extinction Coef-

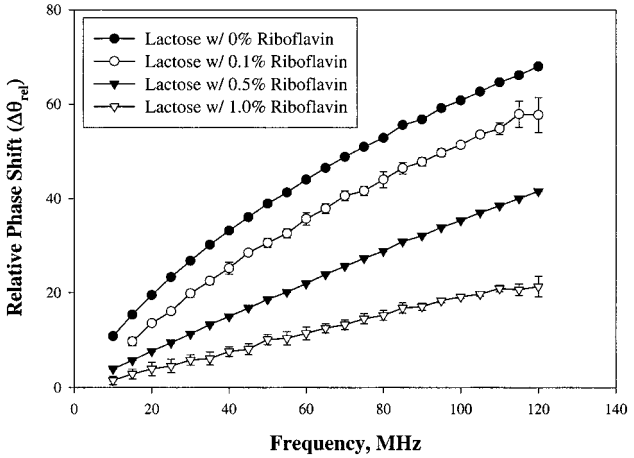

Figure 6—The relative phase shifts of four different lactose–riboflavin powder mixtures plotted at different modulation frequencies. The lactose–riboflavin mixtures are in the same ratios as given in Figure 4 represented by symbols. Measurements were accomplished at 670 nm using a laser diode. Error bars are a result of 10 measurements at each frequency.

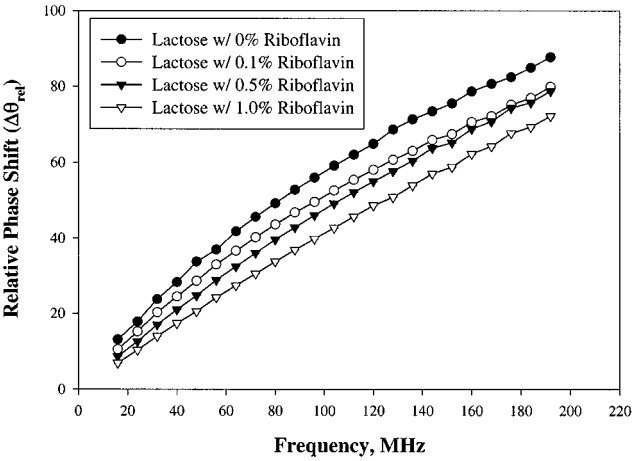

Figure 7—The relative phase shifts of four different lactose–riboflavin powder mixtures plotted at different modulation frequencies. The lactose–riboflavin mixtures are in the same ratios as given in Figure 4 represented by symbols. Measurements were accomplished at 750 nm using a Ti:sapphire laser. Error bars are a result of 10 measurements at each frequency.

ficients of Lactose−Riboflavin Powder Mixtures by FDPM—Again, owing to the sensitivity of FDPM measurements to absorption, measurements at 488 and 515 nm were not possible in the presence of 0.1−1.0% riboflavin. For this reason, we conducted FDPM measurements at a wavelength where riboflavin absorption was small. At these wavelengths, the absorption cross section spectra cannot be accurately measured using conventional attenuation measurements due to low extinction coefficients of the powder mixtures.

Shown in Figure 6 are the relative phase shifts, $\Delta\theta'_{rel}$, for the four different powders at different modulation frequencies measured at 670 nm. Each data point is an average of at least 10 continuous measurements, with the respective error bars as shown in the Figure 6. A steady decrease in the $\Delta\theta'_{rel}$ values is observed at a given modulation frequency with increase in the riboflavin content in lactose. This is expected due to an increase in absorption coefficient by riboflavin. Similar results were obtained for $\Delta\theta'_{rel}$ measurements carried out at 750 and 820 nm as shown in Figures 7 and 8, respectively. A noticeable difference in each of these plots is the magnitude of the change in $\Delta\theta'_{rel}$ as a function of riboflavin content. At higher wavelengths, the change is smaller, indicating lower absorption coefficients of the powder, which can be attributed to lower extinction coefficients for riboflavin. $\Delta\theta'_{rel}$ values at the various frequencies for each wavelength and powder composition were regressed using eqs 5 (reflectance mode) to give the isotropic scattering and absorption coefficients. The absorption coefficients at 670, 750, and 820 nm obtained by regression using eqs 5 are plotted in Figure 9. At 670 nm, the FDPM data for powder mixtures containing 1% riboflavin could not be fit to the solution of the diffusion equation. This may have been due to high absorption levels at this wavelength, which (i) causes significant dampening of the light signal before it can reach the PMT's and (ii) invalidates the diffusion approximation. Nonetheless, for a given wavelength, an increase in the absorption coefficient is observed with increasing riboflavin content in the powder mixtures. Furthermore, the change in absorbance with increasing riboflavin content is greatest at 670 nm, consistent with the largest extinction coefficient value. At longer wavelengths of 750 and 820 nm, the sensitivity drops further, indicating evidence of a reduction of riboflavin extinction coefficients.

If the absorbance due to the lactose constituent is taken to be the *Y*-intercept of the absorbance versus riboflavin content plots, and then its contribution can be subtracted to provide the absorbance owing to riboflavin only. The results plotted in Figure 10 show a linear relationship between the riboflavin absorption coefficient with its concentration in the powder, from which an extinction coefficient can be determined. It is noteworthy that there

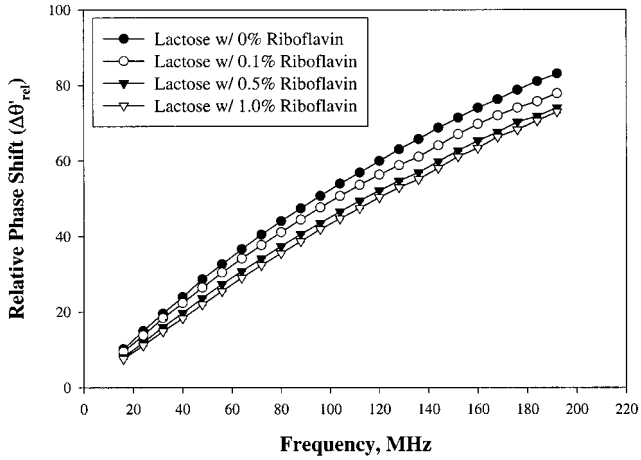

Figure 8—The relative phase shifts of four different lactose–riboflavin powder mixtures plotted at different modulation frequencies. The lactose–riboflavin mixtures are in the same ratios as given in Figure 4 represented by symbols. Measurements were accomplished at 820 nm using a Ti:sapphire laser. Error bars are a result of 10 measurements at each frequency.

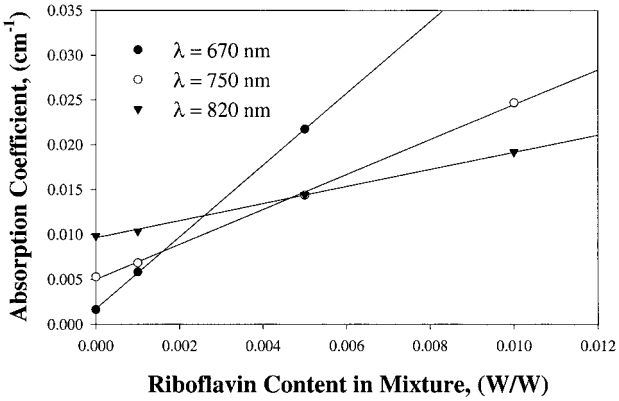

Figure 9—The absorption coefficients for four lactose–riboflavin powder mixtures at three wavelengths, 670, 750, and 820 nm, represented by the three symbols. The absorption coefficients were obtained by regressing the measured relative phase shifts at various frequencies to eq 5.

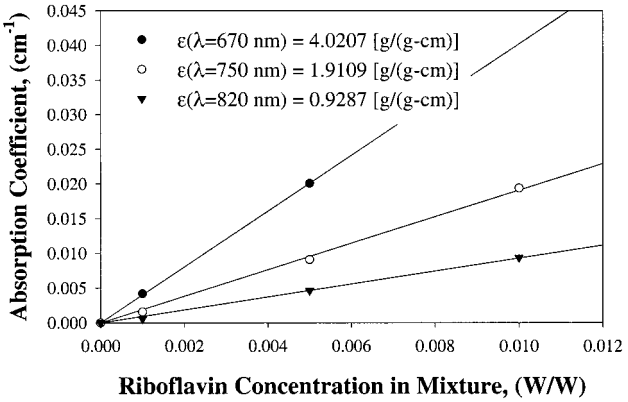

Figure 10—The symbols represent the net absorption coefficients for riboflavin in the four powder mixtures obtained by subtracting the absorption coefficient of pure lactose at each wavelength. The extinction coefficients of riboflavin, shown in the plot, at each wavelength were obtained by regressing the absorption data at the known concentrations using Beer–Lambert's law.

is no significant difference between the extinction coefficients obtained from infinite and reflectance modes of regression of the raw $\Delta\theta'_{rel}$ data. In addition, the riboflavin extinction coefficients are observed to decrease with increasing wavelengths as expected from the UV-spectrophotometer results.

The analysis of the experimental data of the four powder mixtures also yielded the isotropic scattering cross section of the particles. The isotropic scattering coefficients vary from 87 to 123 cm^{-1} for all the four samples at the three wavelengths used, i.e., 670, 750, and 820 nm. The wide range in the measured values may be attributed to the significant polydispersity of the powder mixtures.

6. Conclusions

We have presented FDPM measurements for a simple, two-component powder mixture of riboflavin and lactose. Owing to the sensitivity of FDPM to powder absorbance, we were forced to conduct measurements at wavelengths where riboflavin absorbance did not entirely attenuate the light signal in the powder bed. That is, the measurements were conducted at wavelengths away from the absorbance peaks for the powder mixtures, and the modulated light signal could be detected. At these photon migration wavelengths, the absorbance of riboflavin could not be assessed using conventional attenuation measurements in dilute nonscattering solutions. The results illustrate that for a two-component powder system, the FDPM absorbance increases linearly with riboflavin concentration. The extension to multicomponent mixtures requires additional wavelength sources, but does not require illumination at absorption maxima for maximum sensitivity. Indeed, the ability to detect small absorption cross sections promises applications in low-dose blending operations. Owing to our first principles approach that does not require differential spectroscopy, the variance associated with our analysis should be minimized. Since there is no sampling of powder involved (measurements are made within the powder bed as described herein), there are no sampling variances that need to be assessed. Consequently, the measured variances should be predominantly due to variances associated with the constituents within the powder bed. Finally, since FDPM does not involve *relative* intensity measurements, but rather *absolute* "time-of-flight" phase-delay measurements, there are no measurement errors associated with calibration on an external standard. At the NSF I/UCRC Center in Pharmaceutical Processing at Purdue University we are currently adapting FDPM technology as an in-situ sensor of blend homogeneity.

Nomenclature

Symbols:

c	speed of light in medium (cm/s)
d_1, d_2	source-detector distances (cm)
D	optical diffusion coefficient (cm)
g	average cosine of scattering angles
$\bar{j}(\bar{r},t)$	photon flux (W/m^3)
k	wavenumber (cm^{-1})
k_{real}	real part of k
k_{imag}	imaginary part of k
l^*	isotropic scattering mean free path (cm)
l	thickness of sample (cm)
l_{tr}	transport mean free path of photon (cm)
L	radiance ($W/(m^2\ sr)$)
n	refractive index of the medium
$Q(\bar{r},\hat{s},t)$	photon source term
$\bar{r}$	position vector (cm)
r	radial distance (cm)
$\hat{s},\hat{s}'$	unit vectors in the direction of flux of the photons
$S(\bar{r},t)$	source term

Greek:

$\phi(\bar{r},t)$	isotropic fluence rate (W/m^2)
λ	wavelength of light in media (cm)
μ_a	absorption coefficient (cm^{-1})
μ'_s	isotropic scattering coefficient (cm^{-1})
$\omega/2\pi$	modulation frequency (MHz)
θ'	phase shift angle (radians)
$\Delta\theta'_{rel}$	relative phase-shift (radians)
Ω,Ω'	solid angles of orientation about direction, $\hat{s}$ and $\hat{s}'$ (radians), respectively

References and Notes

1. Muzzio, F. J.; Robinson, P.; Wightman, C.; Brone, D. Sampling Practices in Powder Blending. *Int. J. Pharm.* **1997**, *155*, 153−178.
2. Burger, T.; Kuhn, J.; Caps, R.; Fricke, J. Quantitative Determination of the Scattering and Absorption Coefficients from Diffuse Reflectance and Transmittance Measurements: Applications to Pharmaceutical Powders. *Appl. Spectrosc.* **1997**, *51*, 309−317.
3. Sekulic, S. S.; Ward, H. W.; Brannegan, D. R.; Stanley, E. D.; Evans, C. L.; Sciavolino, S. T.; Hailey, P. A.; Aldridge, P. K. On-line Monitoring of Powder Blend Homogeneity by Near-Infrared Spectroscopy. *Anal. Chem.* **1996**, *68*, 509−513.
4. Cho, J.; Gemperline, P. J.; Aldridge, P. K.; Sekulic, S. S. Effective Mass Sampled by NIR Fiber-Optic Reflectance Probes in Blending Processes. *Anal. Chim. Acta* **1997**, *348*, 303−310.
5. Muhammud, S. A.; Illman, D. L.; Kowalski, B. R. *Chemometrics*; Wiley Publications: New York, 1986.
6. Adams, M. J. *Chemometrics in Analytical Spectroscopy*; Cambridge: England, 1995.
7. Duderstadt, J. J.; Hamilton, L. J. *Nuclear Reactor Analysis*; Wiley Publications: New York, 1976.
8. Davison, B.; Sykes, J. B. *Neutron Transport*; Oxford U. Press: London, 1958.
9. Ishimaru, A. *Wave Propagation and Scattering in Random Media*; Academic Press: New York, 1978, Vol. I.
10. Chandrashekhar, S. *Radiative transfer*; Oxford U. Press: London, 1960.
11. Haskell, R. C.; Svaasand, L. O.; Tsay, T. T.; Feng, T.; McAdams, M. S.; Tromberg, B. J. Boundary Conditions for the Diffusion Equation in Radiative Transfer. *J. Opt. Soc. Am.* **1994**, *11*, 2727−2741.

12. Welch A. J.; van Gemert M. J. C. *Optical-Thermal Response of Laser-irradiated Tissue*; Plenum Publishing Corporation: New York, 1995.
13. Alacala, J. R.; Gratton, E.; Jameson, D. M. A Multifrequency Phase Fluorometer Using the Harmonic Content of a Mode-Locked Laser. *Anal. Instr.* **1985**, *14*, 225−250.
14. Fishkin, J. B.; So, P. T. C.; Cerussi, A. E.; Fantini, S.; Franceschini, M. A.; Gratton, E. Frequency-Domain Method for Measuring Spectral Properties in Multiple-Scattering Media: Methemoglobin Absorption Spectrum in a Tissuelike Phantom. *Appl. Opt.* **1995**, *34*, 1143−1155.
15. Sevick, E. M.; Friscoli, J. K.; Burch, C. L.; Lakowicz, J. R. Localization of Absorbers in Scattering Media by Use of Frequency-Domain Measurements of Time-Dependent Photon Migration. *Appl. Opt.* **1994**, *33*, 3562−3570.

Acknowledgments

The authors are grateful to the NSF I/UCRC Center for Pharmaceutical Processing Research (CPPR) at Purdue University for their material and financial support for conducting this work.

JS990079+